2023 IEEE International Conference on Robotics and Automation (ICRA 2023)
May 29 - June 2, 2023. London, UK

Anthropomorphic robot hand using the principle of sweat and fingerprints of human hands

Donghyun Kim, Junmo Yang and Dongwon Yun*, *Senior Member, IEEE*

Abstract— **In our daily life, when a small amount of sweat or water forms on a person's hand, we can empirically feel that the friction force of the hand increases, and the objects are gripped well. However, if sweat or water forms heavily, we can feel the friction decrease when holding an object. In this study, we analyzed the degree to which fingerprints and sweat present on a person's hand can affect the friction force between the hand and the gripping object. We fabricated an anthropomorphic robot hand with a fingerprint structure to set up an environment similar to that of the human hand, and performed object-holding and friction-change experiments by changing the amount of sweat to verify that this phenomenon can be applied to a robot hand. Furthermore, we for the first time proposed and developed a variable friction system using fluids and microstructures to solve the difficulty of anthropomorphic robot hand force control. By applying the manufactured variable friction system and performing an active friction control performance test and an object grip test of the robot hand, we validated that the fingerprint and sweat of a human hand can affect the grip of an actual object.**

I. Introduction

While traditional grippers are designed to perform repetitive motions, such as those found in assembly line manufacturing, researchers have recently been studying a new type of gripper with a shape more closely resembling that of the human hand. The goal of these grippers is to enable robots to perform more complex, human-like tasks [1-2]. Various studies have been conducted to express the many degrees of freedom of the human hand to improve the anthropomorphic gripper's completeness. Research on driving a finger through a general motor drive and linkage structure is in progress [3-6], and studies on simulating muscles and tendons using new actuating technology are also in progress [7-9]. However, multi-degree-of-freedom drive has a problem in that the size of the driving unit is large compared to the size of the gripper. Some studies were conducted to solve this problem by reducing the complexity and size of the actuator using an under-actuation system [10-13]. First, it is essential to fabricate a sensor for feedback control of the friction control system. Real-time friction force values are crucial for precise force control in the system. Additionally, since the friction control system exhibits varying tendencies with changes in vertical force, a sensor capable of measuring vertical force must also be attached. Developing such a sensing module would allow its application not only to anthropomorphic robot hands but also to various processes requiring a gripper. Despite the many advantages of the under-actuation gripper, it is difficult to conduct force control accurately compared to the conventional gripper. Precise force control is essential for the gripper to perform higher-order tasks. Therefore, prior studies have been conducted to perform precise force control of the under-actuation gripper. [14-15] conducted tactile sensor-based impedance adaptive control to perform stable grip of the under-actuation gripper. [16] studied Model Predictive Control on the under-actuation gripper using vision sensing. [17] performed a theoretical analysis of the actual force of an under-actuation gripper used to conduct force control.

In this paper, we propose a new method of friction control that simulates human fingerprints and sweat that can be added to the existing motor-based force control method. There are prior studies that performed driving and control of robots based on friction force [18-21]. However, these studies only use motor control for friction force control, it is impossible to generate a gripping force that exceeds the motor's natural force. Based on the friction change system which we propose, it is possible to create a robot hand capable of generating forces exceeding the gripping force produced by motor force. [22] has experimentally proven that it is possible to increase or decrease friction according to sweat that forms on fingerprints on real human hands. Generally, when a fluid permeates the area between two objects, the fluid acts as a lubricant to reduce friction. However, in the case of a shape in which the fluid permeates only the empty space while maintaining the contact between the two objects, the frictional force is increased by the attraction between the fluid and the object [23-24]. The fundamental force that increases frictional force via the fluid is intermolecular attraction, and several previous studies analyzed this phenomenon experimentally and theoretically [25-27]. In addition, when the intermolecular force acts over a large area, the increase in frictional force is maximized, thereby creating a significant friction change. In real life, when a small amount of water or sweat forms on hands, we can experience a friction increase. This means that the fingerprint on the hand maximizes the contact area between the fluid and the hand, so that it generates enough force for a person to feel [28-30].

A theoretical analysis of this content was performed in [31], and this paper introduces a robot gripper technology that applies a friction-based force control method with this

This work was supported by the National Research Foundation of Korea(NRF) grant funded by the Korea government(MSIT) (No. 2020R1C1C1012279). *(Corresponding author: Dongwon Yun.)*

Donghyun Kim, Junmo Yang and Dongwon Yun are with the Department of Robotics and Mechatronics Engineering, Daegu Gyeongbuk Institute of Science and Technology (DGIST), Daegu, 42988 South Korea (e-mail: kdhhouse@dgist.ac.kr; longerthanu@dgist.ac.kr; mech@dgist.ac.kr).

principle. There are studies on systems that change gripper surface friction using fluid [32-33]. However, these systems use water to reduce the large friction of the soft gripper, and are different from this paper, which aims at a system that increases and decreases the friction using water.

Section II deals with the overall content of the friction change phenomenon when fluid is present in the fingerprint and the selection of the fingerprint size and shape. Section III contains the contents of making an anthropomorphic robot hand that can attach a selected fingerprint. Section IV shows the results of experiments that change friction by controlling the amount of fluid using the robot hand and fingerprint, and Section V contains the conclusion of this study.

II. Fingerprint Design

A. Friction Force Analysis

It is necessary to analyze the friction change when the fluid is filling in the fingerprint. There are two ways in which a fluid acts to change the friction force between objects, determined by the amount of fluid formed between the objects. When the amount of fluid between the objects is insufficient, the fluid cannot form a layer between the two objects. Instead, the fluid collects in fingerprints, which increases the friction force between the two objects due to the adhesive force caused by the fluid. Adhesive force can be calculated using the work of adhesion, which is the force caused by the intermolecular attraction of an object. The work of adhesion is generally expressed as (1), and is a value for the energy loss when the objects *i* and *j* are detached from the fluid *k*. In previous studies, one of *i* and *j* in this equation was set as a liquid, not a solid [31]. In addition, to calculate (1), it is necessary to distinguish the dispersion force and the polar force of the surface tension of an object, as shown in (2). Based on (2), it is possible to obtain the work of adhesion between a solid and a liquid. (3) shows the work of adhesion between a fluid and an object.

$$\varpi_{ikj} = \gamma_{ik} + \gamma_{jk} - \gamma_{ij}. \quad (1)$$

$$\gamma_{ij} = \gamma_i + \gamma_j - 2\sqrt{\gamma_i^d \gamma_j^d} - 2\sqrt{\gamma_i^p \gamma_j^p}. \quad (2)$$

$$\varpi_{ivj} = 2(\sqrt{\gamma_i^d \gamma_j^d} + \sqrt{\gamma_i^p \gamma_j^p}). \quad (3)$$

In (3), value ϖ_{ivj} represents the work of adhesion between object i and object j. Value γ_i^d and γ_i^p represent the dispersion force and polar force of object i. It is possible to use (3) when objects i and j are liquid or solid; thus, we can obtain the work of adhesion between the fluid and the object through this equation. Work of adhesion affects friction in the same way as surface tension. When moving due to the work of adhesion between two opposing planes, a force is generated in the direction that prevents the movement. We defined this as additional friction force (F_{ad}). This force is proportional to the area of the cross-section of the two objects that meet the fluid, because the more significant the cross-section, the stronger the intermolecular force. This relationship between the additional friction force and the area is linear, and the proportionality constant can be expressed as the work of adhesion. In this paper, based on this principle, we calculate

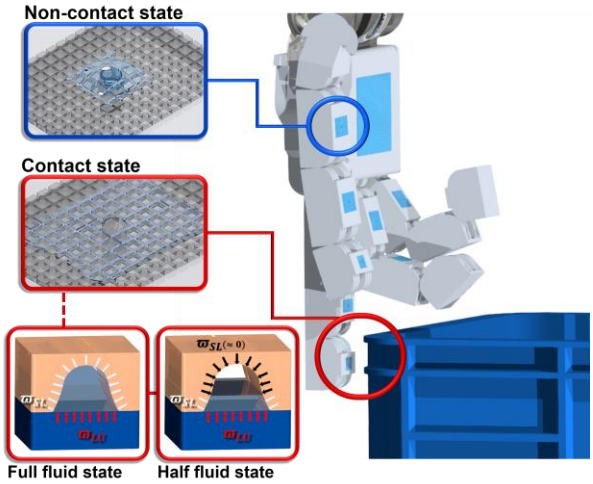

Fig. 1. A conceptual diagram of the adhesive force action method in the presence of water in the fingerprint, and a grid-type structure model.

the amount of added frictional force when there is fluid in the fingerprint. The area where the fluid and the object meet is unclear because the shape of the fingerprint is irregular. Because the shape of the fingerprint is three-dimensional, it is necessary to consider the addition of frictional force on six opposing surfaces. In this paper, we assumed that frictional force is added from the facing surfaces of the upper and lower sides and the opposite side surfaces. The frictional force added by the fluid can be defined as (4). In (4), $\alpha_{adh}, \beta_{adh}$ are values for the area according to the shape and size of the fingerprint. These values are inversely proportional to the distance from the opposite wall and proportional to the area. It can be precisely defined in the case of a flat plane [31], but should be calculated by integrating the reciprocal of the distance to the opposite side when the plane is not regular. Value h_w, h represents the height of the fluid in the fingerprint and the depth of the fingerprint.

$$F_{ad} = \alpha_{adh}\varpi_{LU} + \beta_{adh}(\frac{h_w}{h})\varpi_{SL}. \quad (4)$$

On the other hand, when the fluid creates a thin film between the fingerprint and the object, friction decreases because of the lubrication. Friction force can be calculated based on the case where a thin fluid film occurs. In this case, viscosity causes the frictional force and (5) expresses the force F_v due to the viscosity. Value μ means the viscosity, value A denotes the contact area. Value v is the velocity of the fluid and h means the height of the film. The water film can withstand the normal drag by the surface tension, and the surface tension is inversely proportional to the height of the water film.

$$F_v = \mu A \frac{v}{h}. \quad (5)$$

Friction change due to fluid can always occur in places with narrow valleys such as fingerprints, and this paper proposes a new concept of a robot gripper that can control friction by applying friction change to a gripper. In Fig. 1, we can see how the friction force changes due to the fluid when using the proposed system for a gripper. When spraying water into the fingerprint, the friction force increases in proportion to the amount of water due to the intermolecular force

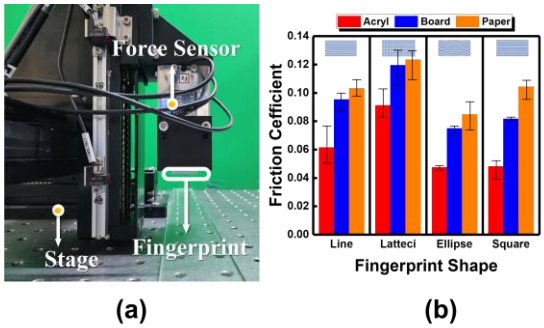

Fig. 2. Experimental settings and results for optimal fingerprint shape selection. (a) Experimental setting. (b) Results of friction coefficient experiments on a total of 4 types of fingerprint shapes (Repeated three times).

between the water and the object. When the height of the fluid in the fingerprint is sufficiently high, the change in width of the contact area decreases due to the surface tension of the fluid, and thus the change width of the additional friction force also decreases. When the fluid fills the inside of the fingerprint, a fluid film is formed outside the fingerprint and the friction force decreases sharply. We manufactured a fingerprint to lay the foundation for force control by implementing this hypothesis on the gripper.

B. Fingerprint selection & Fabrication

We conducted experiments to find the optimal shape of fingerprint to be attached to the gripper. We first selected four fingerprint shapes and tried to find the best fingerprint among the four shapes. We conducted experiments to obtain the friction coefficient for various materials and fingerprints and selected the fingerprint shape with the highest friction coefficient. Fig. 2 (a) shows the experimental setup. After attaching a fingerprint to a two-axis linear stage (AM1-0401, MISUMI Corp, Tokyo, Japan) and bringing the fingerprint into contact with the ground, we measured the friction force when moving the fingerprint in a direction parallel to the ground. We measured friction force and normal force using a three-axis load cell (CMAS111, CAS, South Korea) attached to the fingerprint and carried out the experiment by moving the stage in both directions. The friction coefficient value was derived using the normal force and friction force measured in each experiment and performed three experiments on the same material for data reliability. Result of the friction coefficient experiment is shown in Fig. 2 (b). As a result, we confirmed that the lattice-shaped fingerprint had the largest friction coefficient for all objects. This is because the coefficient of friction increases with the roughness of the surface shape, and the lattice is the roughest shape. In addition, lattice -type fingerprints were selected in this paper because lattice -type fingerprints are more suitable than other fingerprints to facilitate fluid.

The size of the fingerprint is 0.3mm wide and 0.4mm deep. To make such a small shape with flexible material, we shaped and hardened flexible silicone. In this study, we made all of the flexible fingerprints in this way. The mold was manufactured using a 3D printer, Objet 30 Pro (Stratasys, USA), which uses a polyjet printing method, to make a mold of the exact size and shape. We produced a flexible material fingerprint using MMH-1K (hardness 40, MoldMaster, South

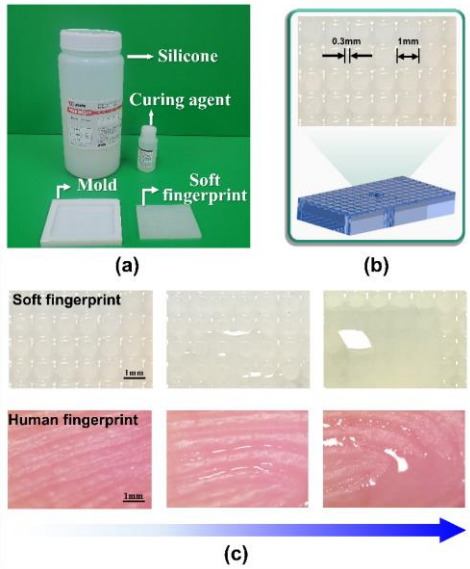

Fig. 3. (a) Molding silicone and fingerprint-shaped mold required for fingerprint production. (b) Actual photograph of the produced fingerprint. (c) Comparison of shapes of fabricated fingerprint and actual fingerprint.

Korea), a condensed flexible silicone. Fig. 3 (a) shows the fabrication process and Fig. 3 (b) shows the shape of the fingerprint. As a result of comparing the fabricated silicone fingerprint with the fingerprint of an actual finger, as shown in Fig. 3 (c), if a small amount of liquid is present, the liquid penetrates into the interior of the fingerprint. However, when an excessive amount of liquid is present, it can be confirmed that the liquid does not penetrate into the interior of the fingerprint due to the surface tension.

III. Development of the Robot Hand

We evaluated the proposed system with a gripper attached with a variable friction module consisting of a soft fingerprint capable of water jetting. While it is possible to assess the proposed system's performance using different gripper types, this study focused on evaluating the system using an under-actuated anthropomorphic robot hand. The fabricated robot hand is typically challenging to control the force, and its efficacy was verified by attaching the proposed friction change system to it. By doing so, we were able to assess the system's impact on the robot hand's control and functionality.

A. *Robot Hand Fabrication*

The manufactured robot hand consists of four fingers: a thumb, index, middle, and ring; each finger has three degrees of freedom. There are two types of joint. First, there is a general one degree of freedom rolling joint, which is used for all fingers except the thumb. Because the carpometacarpal (CMC) joint of the thumb in the human hand is the only joint for which the direction of the axis of rotation is not fixed, only the CMC joint of the robot hand thumb has a different joint shape. In this paper, we made a joint in which the driving direction and the tendon direction are orthogonal and used this joint as the robot hand's thumb CMC joint.

Fig. 4 shows the shape of the two types of joints. Both joints are rolling joints. In the case of joint 1, both links of the rolling joint have a cylindrical shape, so the direction of the

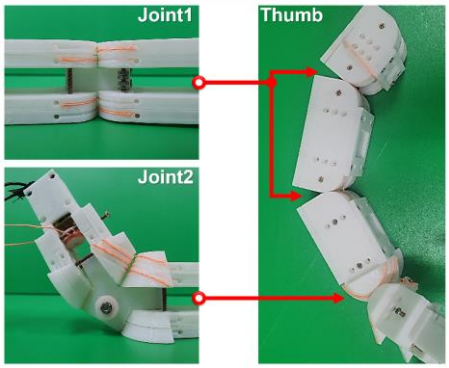

Fig. 4. Actual photos of the two types of joints and the shape of the gripper thumb made using the corresponding joints. Both joint1 and joint2 are rolling joints, and rotation is constrained in only one direction by a wire that performs ligament mechanics.

rotation axis can always be kept constant. In the case of joint 2, both links of the rolling joint have a cone shape, and the direction of the rotation axis can be changed at any time according to the rotation angle, so that the joint can create more various angles of movement. To reduce the degree of freedom of the joint that can be moved by simple rotation and slip, we used four fixing wires, and joints having only 1 degree of freedom in the form of simple rotation were manufactured using tension applied to the wires. The overall shape of the fabricated robot hand can be seen in Fig. 5.

Robotic expression of the human hand's finger movements can be challenging due to the lack of independent motion in each joint or finger. In this study, we utilized the under-actuation method using wire as the driving mechanism, similar to those found in grippers, to mimic human hand characteristics. Typically, additional components such as springs are used to restore joints to their initial position after under-actuation. However, the use of these parts increases the gripper's overall size. To address this issue, we employed wires that could drive rotation in both directions, allowing for bi-directional movement with a single motor and avoiding the need for additional components.

B. Fluid Spraying System

We made a space for soft material fingerprints to be placed along the gripper's entire gripping area to attach the fingerprint system. To inject the fluid into the fingerprint, we used a rubber hose with a diameter of 3 mm, a system that allows fluid to permeate into the fingerprint through tiny holes such as pores. Fingerprint production was carried out with the same material as in Figure 3. During the molding process, a 3mm hose was inserted in the middle to penetrate the center of the fingerprint, creating a space for a hole (Fig. 6(a)). After molding, we attached the hose and silicone to be used for actual water injection using rubber adhesive (Permabond, Italy). Fig. 6 (b) shows the system. To spray the fluid onto the fingerprint, we used Fusion 200 Touch (Revodix, South Korea), a micro pump product that can spray small amounts of fluid and water simultaneously in several directions through a hose. In Fig. 6 (c), it is possible to check the connection forms of the micro pump, syringe, and hose.

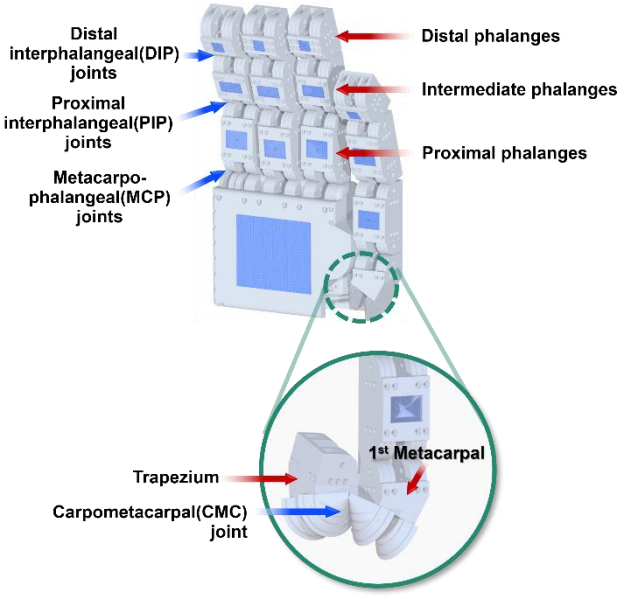

Fig. 5. Manufactured anthropomorphic robot hand.

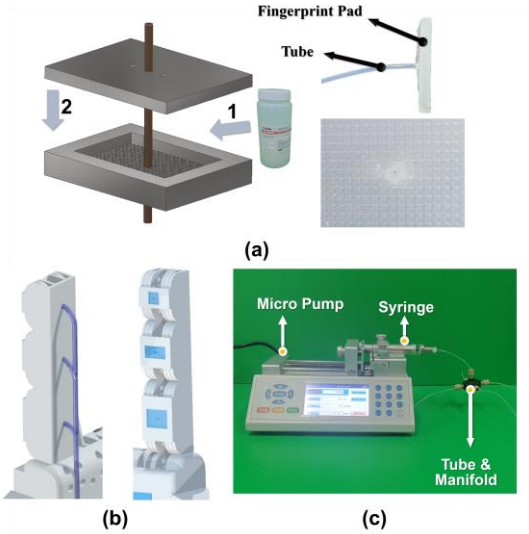

Fig. 6. (a) Hole design in fingerprint pad and hose attachment method. (b) System concept diagram that makes a way for the fluid to permeate into the silicone and allows the fluid to permeate the fingerprint in the contact state during injection. (c) Photo showing the attachment form of micro pump, syringe, and tube.

IV. Experiments and Evaluations

We conducted experiments to observe changes in frictional force when gripping an actual object using the manufactured gripper and variable friction module. Two types of gripping experiments were conducted according to the tendency of friction change. The manufactured robot hand can grip objects of various sizes, weights, and materials, but in this experiment, a plastic reagent bottle that sufficiently contacts the fingerprint of the robot hand when gripping was selected to maximize friction change. After selecting an applied voltage that can produce an appropriate gripping force according to the purpose of the experiment, we measured the maximum weight that the robot hand can grip when each applied voltage is applied. The maximum weight was measured by adding weights and small nuts to the plastic

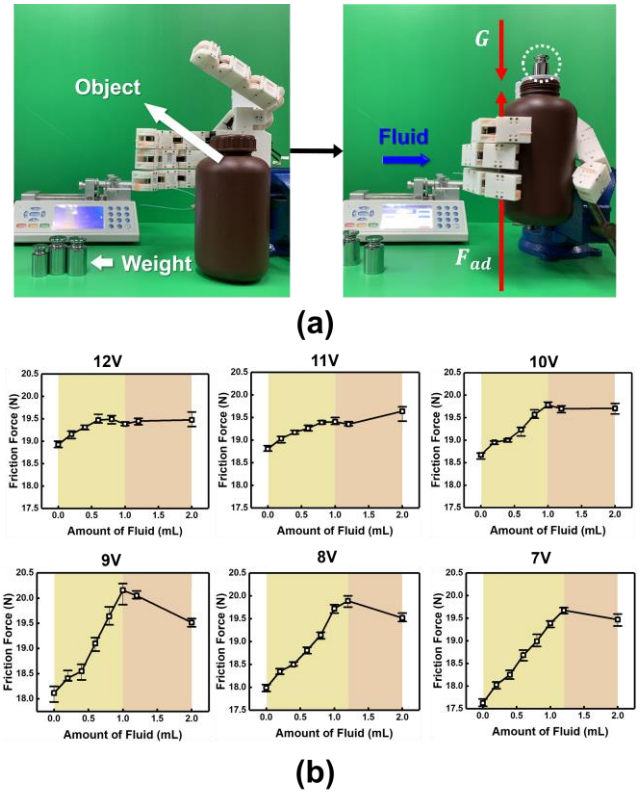

Fig. 7. (a) Experimental setting for measuring the gripping force of the robot hand according to the amount of water. (b)Variable friction system verification experiment performed by changing the force. The experiment was conducted by changing the grip force of the robot hand; the experiments were repeated 5 times.

reagent bottle, and the experimental setting process can be seen in the Fig. 7 (a).

Through these experiments, we implemented a friction control system based on water spray, and conducted other experiments to show the possibility that this system could be used in real situation. First of all, it has been shown through experiments that grasping and placing objects is possible without voltage change using the reagent bottle used in the previous experiment. In addition, an experiment was conducted to apply a friction increase system and a friction decrease system to glass bottles and thin plastic cup that are easy to breakage and deformation.

A. Friction Increase Experiment

The first experiment investigated the increase in gripping force when fluid is sprayed on the fingerprint. To proceed with the experiment, we conducted the grasping experiment by varying the voltage of the actuator. Through this experiment, it is possible to observe the relationship between the amount of fluid injected and the gripping force of the actuator. This experiment shows the possibility of performing force control of a real gripper via a variable friction module. Fig. 7 (b) shows the results of the experiment.

Based on the results of this experiment, we can see that the tendency of frictional force change due to water jetting is similar even when the applied voltage is changed. It can be seen that friction increases when 2.0mL of water is injected only in the 11V graph of Fig. 7 (b). This is because the grip angle of the gripping object was optimally formed at 11V, and

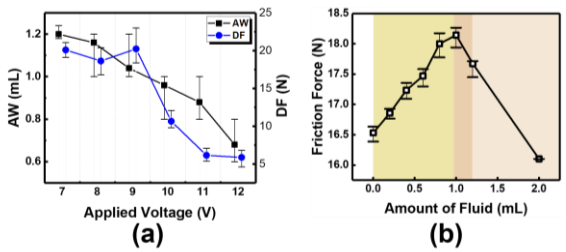

Fig. 8. (a) Analysis of the amount of additional frictional force and the amount of water required according to the change in force. (b) Experiment to confirm the rapid decrease in friction in which the grip force of the motor is set to the minimum range for gripping. Each experiment was repeated 5 times.

the amount of water that can be injected increased. The frictional force increases according to the amount of water sprayed, and when the amount of fluid exceeds a specific value, the frictional increase phenomenon disappears. There are two characteristics that can be observed when the applied voltage is increased.

First, there is a difference (Difference of friction force, DF) between the minimum friction state without spraying water according to the applied voltage and the maximum friction state value in which friction is increased to the maximum by spraying water. When the applied voltage increases, the DF value tends to decrease. In addition, the amount of sprayed water (Amount of Water, AW) when the friction is increased to the maximum friction state tends to decrease as the magnitude of the applied voltage increases.

Fig. 8 (a) shows these two results. As the applied voltage increases, the volume of the space between the fingerprint and the object decreases because the pressure applied to the soft fingerprint increases. Thus, the maximum amount of water that can be injected (AW) and the amount of frictional force that increases (DF) also decreases. In other words, the friction characteristics change when the gripping force of the actuator changes. Based on this result, it can be seen that the friction control system can replace force control in a system in which normal force measurement is possible.

Based on the results shown in Fig. 8 (a), we can also check the effectiveness of the proposed friction control system. In general, the relationship between the force of the under-actuation gripper and the force of the actuator cannot be precisely specified because it depends on the shape of the gripper. Therefore, only rough control becomes possible when using actuator-based force control. In Fig. 7 (b), where the difference between the applied voltage of 7V and the applied voltage of 12V is not significant (10%), we can see the disadvantage of the under-actuation gripper. In this experiment, the friction force increase by water spraying was about 0.25N, and the difference in the friction force when the minimum applied voltage and the maximum applied voltage is applied is about 1.3N. The results demonstrate that implementing fluid-based force control is a more efficient approach than controlling the actuator force for regulating the force of a robot hand during operation.

B. Friction Decrease Experiment

The second experiment attempted to view the slip phenomenon, because of lubrication. In general, the slip phenomenon does not appear when the force of the actuator

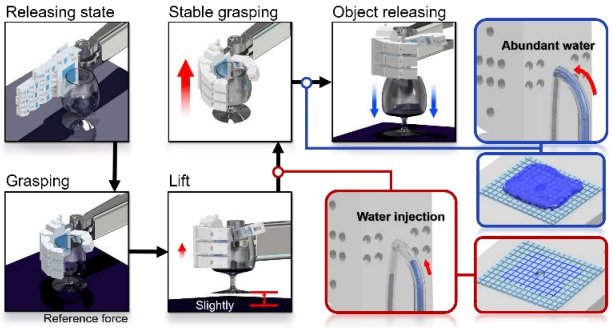

Fig. 9. Conceptual diagram of pick and place process for high-risk products with variable friction system applied.

is strong; it appears only with force sufficient to form a water film between the gripper and the object. This friction decrease system has the advantage of maximizing efficiency in industrial processes. As in the previous experiment, we attempted to find the applied voltage value (4.8V~5.4V) that yielded an appropriate gripping force to create a friction force decrease system. Fig. 8 (b) shows the results of this experiment.

Based on the results of the second experiment, when the amount of water sprayed is excessive, we can observe that the friction force rapidly decreases, as shown in Fig. 8 (b). This is the same phenomenon as the rapid decrease in friction force [31]. This rapid friction force decrease phenomenon can significantly broaden the boundary of use of the friction change module. If the friction change system applies not only the function of increasing friction but also the phenomenon of sharp decrease in friction, it is possible to grip more diverse objects. For example, the gripper should go through a precision control system to handle the processing of easily breakable objects, which is a complex way for an anthropomorphic robot hand to perform. The variable friction module can create a simplified control scheme by implementing the anthropomorphic robot hand fabricated in this study, as shown in Fig. 9.

C. Cylindrical Objects Grasping Experiment

Based on the results of the previous experiment, we can assume that the increase in friction was maximized when a total of 1.0 mL fluid was sprayed on the fingerprint of the robot hand and that the friction decrease would occur rapidly when 2.0 mL fluid was sprayed. We performed a grasping experiment using a friction change system on a glass beaker and thin plastic cup, which are easily damaged and deformable objects. We measured the maximum grasping weight when the fluid is not sprayed, when 1.0mL of water is sprayed, and when 2.0mL of water is sprayed by changing the applied voltage. The result is shown in Fig. 10.

The graph in Fig. 10 (a) shows the results of the grasping experiment using a glass beaker. As with the experiment using a plastic reagent bottle, we measured the maximum gripping force while adding weight to a glass beaker. When the applied voltage was 9V, which is the minimum value that can grip the object, the gripping force increased by 2.8N when using the friction increase system, and when the applied voltage was 15V, the gripping force increased by 1.1N. It can be confirmed that the friction increase system operates, and

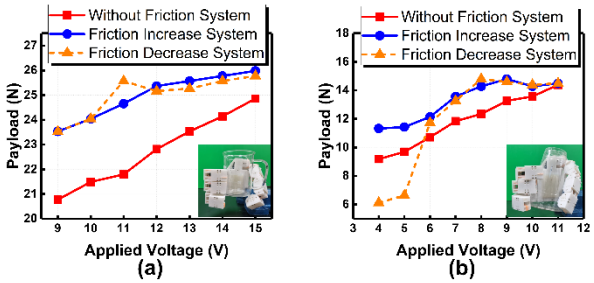

Fig. 10. Results of cylindrical objects grasping experiment. (a) Glass Beaker grasping experiment. (b) Plastic Cup grasping experiment.

the friction change decreases as the applied voltage increases. In other words, it is possible to reduce the risk of damage due to excessive applied voltage by using the friction increase system.

The graph in Fig. 10 (b) shows the results of a gripping experiment using a plastic cup, which is an atypical object. The experiments were conducted in the same way. In this experiment, the DF was measured from a maximum of 2.2N to a minimum of 0.1N. The difference in gripping force decreases as the applied voltage increases, similar to that of other objects, but it was confirmed that the effect of the friction increase system almost disappeared when the applied voltage exceeded 10N. The reason is that the plastic cup is deformed by the pressure of the finger, and the friction control system does not work.

When a large pressure is applied to an object and deformation occurs, it can be supplemented by using a friction increase system, and placing process can be performed without unnecessary motor control through the friction decrease system.

V. Conclusion

This study revealed that fingerprints and sweat contribute to the frictional force in the human hand and, using flexible material, we made a fingerprint similar to the shape of a human fingerprint and created a fluid injection system to simulate a human fingerprint. In addition, we first proposed and manufactured an anthropomorphic robot hand grafted with a variable friction system and showed that it is possible to use the friction control system significantly in fields requiring force control. Our study demonstrated that the variable friction system is more efficient than force control using an actuator. In addition, it was found to be possible to implement not only a friction increase system, but also a friction decrease system, which can dramatically increase the field of use of the friction control system. Several future plans remain for the practical use of the friction control system.

First, it is essential to fabricate a sensor for feedback control of the friction control system. Real-time friction force values are crucial for precise force control in the system. Additionally, since the friction control system exhibits varying tendencies with changes in vertical force, a sensor capable of measuring vertical force must also be attached. Developing such a sensing module would allow its application not only to anthropomorphic robot hands but also to various processes requiring a gripper.

REFERENCES

[1] S. MIN AND S. YI, "DEVELOPMENT OF CABLE-DRIVEN ANTHROPOMORPHIC ROBOT HAND." *IEEE ROBOTICS AND AUTOMATION LETTERS* 6.2 (2021): 1176-1183.

[2] J. Yang, J. Kim, D. Kim and D. Yun, "Shock Resistive Flexure-Based Anthropomorphic Hand with Enhanced Payload." *Soft Robotics* (2021).

[3] M. A. A. Wahit, S. A. Ahmad, M. H. Marhaban, C. Wada, and L. I. Izhar, "3d printed robot hand structure using four-bar linkage mechanism for prosthetic application." *Sensors (Basel, Switzerland)* 20.15 (2020).

[4] H. Yang, G. Wei, L. Ren, Z. Qian, K. Wang, H. Xiu, and W. Liang, "A low-cost linkage-spring-tendon-integrated compliant anthropomorphic robotic hand: MCR-Hand III." *Mechanism and Machine Theory* 158 (2021): 104210.

[5] Z. Xu, and E. Todorov, "Design of a highly biomimetic anthropomorphic robotic hand towards artificial limb regeneration." *2016 IEEE International Conference on Robotics and Automation (ICRA)*. IEEE, 2016.

[6] Tian, Li, et al. "Towards complex and continuous manipulation: A gesture based anthropomorphic robotic hand design." *IEEE Robotics and Automation Letters* 6.3 (2021): 5461-5468.

[7] V. Ryabchevsky, A. Nikonov, and G. Nikonova, "Development of Pneumatic Artificial Muscles and an Anthropomorphic Gripper Control Module." *2021 International Siberian Conference on Control and Communications (SIBCON)*. IEEE, 2021.

[8] D. Gong, L. Hao, J. Yu, and G. Zuo, "Bionic design of a dexterous anthropomorphic hand actuated by antagonistic PAMs." *2020 IEEE International Conference on Real-time Computing and Robotics (RCAR)*. IEEE, 2020.

[9] P. Ohta, et al. "Design of a lightweight soft robotic arm using pneumatic artificial muscles and inflatable sleeves." *Soft robotics* 5.2 (2018): 204-215.

[10] I. Hussain, et al. "Modeling and prototyping of an underactuated gripper exploiting joint compliance and modularity." *IEEE Robotics and automation letters* 3.4 (2018): 2854-2861.

[11] A. Firouzeh, and J. Paik, "Grasp mode and compliance control of an underactuated origami gripper using adjustable stiffness joints." *Ieee/asme Transactions on Mechatronics* 22.5 (2017): 2165-2173.

[12] K. Lee, Y. Wang, and C. Zheng, "Twister hand: Underactuated robotic gripper inspired by origami twisted tower." *IEEE Transactions on Robotics* 36.2 (2020): 488-500.

[13] N. Tan, X. Gu, and H. Ren, "Simultaneous robot-world, sensor-tip, and kinematics calibration of an underactuated robotic hand with soft fingers." *IEEE Access* 6 (2017): 22705-22715.

[14] Z. Y. Chu, S. B. Yan, J. Hu, and S. Lu, "Impedance identification using tactile sensing and its adaptation for an underactuated gripper manipulation." *International Journal of Control, Automation and Systems* 16.2 (2018): 875-886.

[15] M. V. Liarokapis, B. Calli, A. J. Spiers, and A. M. Dollar, "Unplanned, model-free, single grasp object classification with underactuated hands and force sensors." *2015 IEEE/RSJ International Conference on Intelligent Robots and Systems (IROS)*. IEEE, 2015.

[16] B. Calli, and A. M. Dollar, "Vision-based model predictive control for within-hand precision manipulation with underactuated grippers." *2017 IEEE International Conference on Robotics and Automation (ICRA)*. IEEE, 2017.

[17] A. Kobayashi, et al. "Analysis of precision grip force for uGRIPP (underactuated gripper for power and precision grasp)." *2017 IEEE/RSJ International Conference on Intelligent Robots and Systems (IROS)*. IEEE, 2017.

[18] J. Ha, G. Fagogenis, and P. E. Dupont, "Modeling tube clearance and bounding the effect of friction in concentric tube robot kinematics." *IEEE Transactions on Robotics* 35.2 (2018): 353-370.

[19] C. Ren, X. Li, X. Yang, and S. Ma, "Extended state observer-based sliding mode control of an omnidirectional mobile robot with friction compensation." *IEEE Transactions on Industrial Electronics* 66.12 (2019): 9480-9489.

[20] J. Li, W. Chang, and Q. Li, "Soft robot with a novel variable friction design actuated by SMA and electromagnet." *Smart Materials and Structures* 27.11 (2018): 115020.

[21] K. Guo, Y. Pan, and H. Yu, "Composite learning robot control with friction compensation: a neural network-based approach." *IEEE Transactions on Industrial Electronics* 66.10 (2018): 7841-7851.

[22] T. André, P. Lefèvre, and J. L. Thonnard, "A continuous measure of fingertip friction during precision grip." *Journal of neuroscience methods* 179.2 (2009): 224-229.

[23] E. Koren, et al. "Adhesion and friction in mesoscopic graphite contacts." *Science* 348.6235 (2015): 679-683.

[24] B. Luan, and R. Zhou, "Wettability and friction of water on a MoS2 nanosheet." *Applied Physics Letters* 108.13 (2016): 131601.

[25] M. Cheng, M. Song, H. Dong, and F. Shi, "Surface adhesive forces: a metric describing the drag-reducing effects of superhydrophobic coatings." *Small* 11.14 (2015): 1665-1671.

[26] Z. Pawlak, W. Urbaniak, and A. Oloyede, "The relationship between friction and wettability in aqueous environment." *Wear* 271.9-10 (2011): 1745-1749.

[27] F. L. Leite, et al. "Theoretical models for surface forces and adhesion and their measurement using atomic force microscopy." *International journal of molecular sciences* 13.10 (2012): 12773-12856.

[28] M. J. Adams, et al. "Finger pad friction and its role in grip and touch." *Journal of The Royal Society Interface* 10.80 (2013): 20120467.

[29] L. C. Gerhardt, et al. "Influence of epidermal hydration on the friction of human skin against textiles." *Journal of the Royal Society Interface* 5.28 (2008): 1317-1328.

[30] S. Kondo, and H. Hasegawa, "Sweat Absorption Reduces the Frictional Force Between a Finger Pad and the Surface of a Flat Plate." *ITE Transactions on Media Technology and Applications* 5.1 (2017): 17-23.

[31] D. Kim, and D. Yun, "A study on the effect of fingerprints in a wet system." *Scientific Reports* 9.1 (2019): 1-10.

[32] T. Nishimura, et al. "Soft robotic hand with finger-bending/friction-reduction switching mechanism through 1-degree-of-freedom flow control." *IEEE Robotics and Automation Letters* 7.2 (2022): 5695-5702.

[33] K. Mizushima, T. Nishimura, Y. Suzuki, T. Tsuji and T.Watanabe, "Surface Texture of Deformable Robotic Fingertipsfor a Stable Grasp Under Both Dry and Wet Conditions," *IEEE Robotics and Automation Letters*, vol. 2, no. 4, pp.2048-2055.